SUPPLEMENTAL DATA

Equipment and HPLC Methods

HPLC purification was performed using a Merck-Hitachi L-7100 HPLC pump and a Waters μ-Bondapak C18 column (7.8 x 300 mm, 10 μm). A Pharmacia UV-1 absorbance detector (λ = 254 nm) and a custom-built ionization chamber for the detection of radioactivity were used. The HPLC eluent was 0.01 M H_3PO_4/CH_3CN (77/23, v/v), and the flow rate was 8 mL/min.

To determine the radiochemical and chemical purity of the synthesized molecules, analytical HPLC was performed using a Hitachi L-2130 HPLC pump, a Symmetry C18 column (5 μm, Waters), a Hitachi L-2400 UV detector (λ = 246 nm), and a 2 x 2 inch NaI-crystal (Wallac RD 1361) for the detection of radioactivity. An L-7100 HPLC pump, a Symmetry C18 column, and a Merck-Hitachi D-7400 UV detector (λ = 246 nm) were used to measure the concentration of ORM-13070. The eluent was 0.05 M H_3PO_4/CH_3CN (83/17; v/v), and the flow rate was 2.0 mL/min.

Quality of ^{11}C-ORM-13070

The amount of radioactivity, the pH, and the volume of the end product were recorded. The identity, radiochemical purity, and concentration of the tracer were determined using the analytical HPLC systems described above. The concentrations of ORM-13070 and its precursor ORM-13333 were determined using reference standards. The radiochemical yield was calculated from the initial amount of ^{11}C-methane, and decay-corrected to end of bombardment (EOB). The specific activity (SA) of the product is reported to end of synthesis (EOS).

Supplemental Table 1. Uptake of ^{11}C-radioactivity in organs of interest of Sprague-Dawley rats at various time points after injection of ^{11}C-ORM-13070. Values are expressed as %ID/g tissue (means ± SD).

Organ/tissue	2 min (n=3)	5 min (n=3)	10 min (n=3)	20 min (n=3)	40 min (n=3)
Brain	5.3±1.1	1.76±0.23	0.55±0.22	0.32±0.04	0.19±0.02
Adrenal glands	13.2±3.5	2.96±0.74	1.10±0.34	0.81±0.05	0.50±0.05
Lungs	6.27±0.90	0.93±0.09	0.35±0.07	0.33±0.02	0.23±0.04
Heart	3.98±0.92	0.56±0.14	0.28±0.07	0.24*	0.16±0.01
Thyroids	2.5±1.2	0.83±0.21	0.58±0.37	0.55±0.15	0.31±0.03
Thymus	1.79±0.47	1.14±0.16	0.38±0.17	0.31±0.02	0.18±0.01
Kidneys	1.74±0.35	0.76±0.10	0.37±0.12	0.32±0.02	0.26±0.02
Small intestine	1.31±0.56	2.16±0.35	2.8±1.4	6.2±2.7	5.7±2.0
Pancreas	1.05±0.57	1.41±0.32	0.55±0.21	1.4±1.4	0.37±0.07
Erythrocytes	0.82±0.23	0.18±0.05	0.08±0.03	0.09*	0.07±0.02
Blood	0.81±0.22	0.18±0.02	0.10±0.03	0.12±0.02	0.09±0.02
Plasma	0.90±0.19	0.23±0.03	0.12±0.04	0.13±0.01	0.11±0.02
Liver	0.86±0.13	1.65±0.34	1.13±0.33	1.33±0.02	0.82±0.12
Salivary	0.79±0.32	1.17±0.20	0.66±0.29	1.04±0.15	0.95±0.30
Large intestine	0.35±0.34	0.37±0.08	0.23±0.09	0.42±0.08	0.41±0.19
Stomach	0.28±0.08	1.03±0.59	0.58±0.18	1.69±0.68	1.25±0.50
Testes	0.26±0.04	0.33±0.06	0.21±0.11	0.25±0.01	0.16±0.01
Bone marrow	0.21±0.03	0.44±0.05	0.42±0.14	0.50±0.05	0.24±0.08
Spleen	0.11±0.05	0.37±0.05	0.19±0.05	0.22±0.07	0.13±0.02
Bone	0.10±0.03	0.07±0.01	0-04±0.02	0.04±0.02	0.06±0.03
Skin	0.07±0.04	0.16±0.02	0.12±0.08	0.20±0.02	0.21±0.05
Muscle	0.06±0.03	0.18±0.01	0.15±0.09	0.18±0.02	0.12±0.01
Fat	0.04±0.01	0.13±0.04	0.12±0.01	0.27±0.10	0.28±0.03

* n=1

Supplemental Figure 1. Representative ex vivo autoradiographic ^{11}C-ORM-13070 images of striatal (left) and cerebellar (right) cryosections of non-treated control animals (at 10 min and 30 min post injection) and of a Sprague-Dawley rat pre-treated with atipamezole (ATI; 30 min post injection).

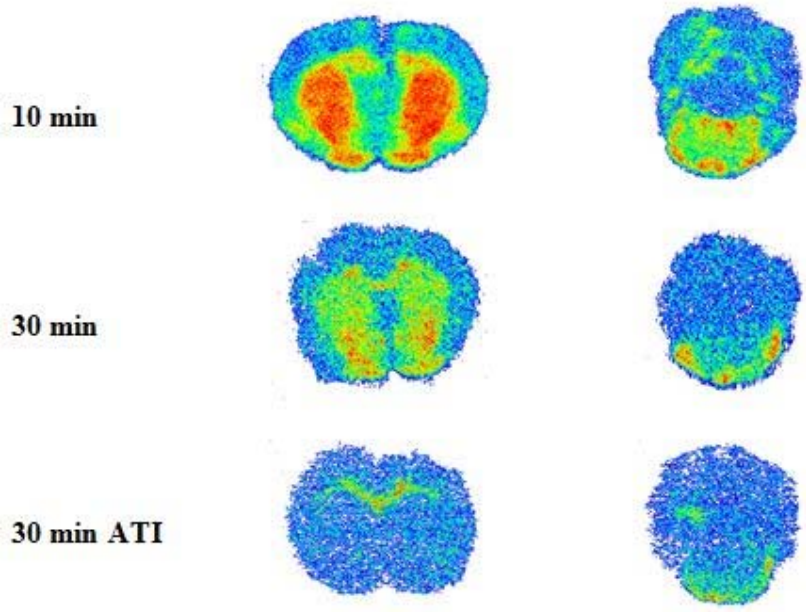

Supplemental Figure 2. Representative ex vivo autoradiographic ^{11}C-ORM-13070 images of brain sections from α_{2A}-knock-out, α_{2AC}-knock-out and wild-type mice, at 10 min post injection.

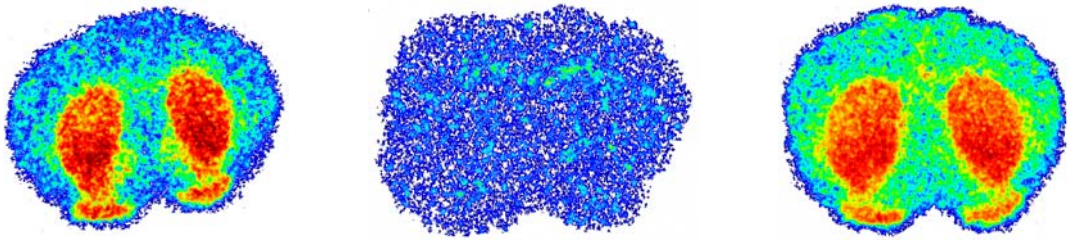

α_{2A}-KO **α_{2AC}-KO** **WT**

Metabolite Analysis with HPLC

^{11}C-ORM-13070 and its radioactive metabolites were analyzed in rat plasma, striatum, and cerebellar cortex using radio-HPLC with a semi-preparative μ-Bondapak C18 column. Two 3 x 3 inch NaI-crystals (Bicron Inc.), connected in coincidence for detection of the annihilation radiation of β^+-particles, were used to detect the radioactivity on the outflow of the column. The mobile phase flow rate was 6 mL/min. From 0 to 3 min, the mobile phase composition was constant at 15% acetonitrile and 85% 0.05 M acetic acid. A linear gradient from 15 to 60% acetonitrile was applied from 3 to 7 min. From 7 to 8 min, the mobile phase composition returned to 15% acetonitrile and 85% 0.05 M acetic acid, and remained the same until the end of the run. The total analysis time was 10 min.

Metabolite Identification with Mass Spectroscopy

Attempts were made at the Drug Metabolism Laboratory of Orion Pharma to identify the two radiometabolites formed from ^{11}C-ORM-13070. Rats were dosed with non-radioactive ORM-13070 (3 mg/kg) together with an equal amount of ORM-13070 containing $^{13}C^{2}H_3$ in the methyl group corresponding to the ^{11}C-label in ^{11}C-ORM-13070. This stable isotope-containing $^{13}C^{2}H_3$-ORM-13070 was employed to facilitate metabolite identification, as it was expected to be metabolised in a similar manner as ^{11}C-ORM-13070.

Samples of plasma and brain were collected and pre-treated with protein precipitation prior to analysis with an LC-MS/MS system consisting of an UPLC separations module (Waters Acquity®) and high-resolution Q-TOF Synapt™ G2 mass spectrometer (Waters) using positive (ESI+) electrospray ionisation. The acquired raw data were processed with MassLynx™ software version 4.1 and MetaboLynx™ software version 4.1 in order to identify expected and unexpected metabolites.

Protein-precipitated plasma and brain samples were also fractionated with an HPLC-UV system. A peak corresponding to M1 could not be detected with the employed UV wavelength (244 nm), but relevant fractions were collected according to their retention time, evaporated to dryness, dissolved in MS-compatible solvent and analysed with the UPLC-MS method described above. Dissolved fractions were also infused directly into a high resolution Orbitrap XL mass spectrometer (Thermo Fisher Scientific) using a TriVersa NanoMate (Advion Inc.) chip-based electrospray ion source. Both positive (ESI+) and negative (ESI-) electrospray ionisation was used and data were collected for extended periods of time in order to enable all ionisable compounds in the sample to become visible in the MS spectrum.

Metabolites corresponding to M1 and M2 could not be detected in plasma or brain samples with any of the employed mass spectrometry methods. Any metabolite containing the methyl group of $^{13}C^{2}H_3$-ORM-13070 would have had a characteristic +4 amu pattern in its MS spectrum. This feature was utilised in the search for metabolites. Since no such metabolites were detected, it is considered likely that M1 and M2 represent volatile compounds with low molecular weight, not detectable with the employed HPLC-MS approaches.

In primary hepatocyte incubation assays in vitro, demethylation has been found to be the major metabolic pathway of ORM-13070. Over 30% of the metabolites formed did not contain the methyl group. Other major metabolites were different hydroxylation products that were subsequently conjugated to form sulpho- or glucuronide metabolites (data on file, Orion Pharma). None of the major metabolites formed could be identified as M1 or M2. Radioactive M1 was found as a very intensive peak compared to the parent peak in rat plasma after administration of ^{11}C-ORM-13070, which suggests that M1 was a major metabolite (data on file, Orion Pharma). It is concluded that the major radioactive metabolite M1 is likely to be a small volatile compound with no affinity for the target receptor, and therefore unlikely to interfere with the interpretation of the PET results obtained with ^{11}C-ORM-13070.

Supplemental Figure 3. HPLC chromatograms of samples from rat striatum, cerebellum and plasma at 10 min after ^{11}C-ORM-13070 injection. The retention times for ^{11}C-ORM-13070, metabolite 1 and metabolite 2 were 7.3 min, 2.1 min and 3.4 min, respectively.